

Design of a Sliding Controller for Optical Disk Drives

Yu-Sheng Lu, Chung-Hsin Cheng, Shuen-Shing Jan

Abstract—This paper presents the design and implementation of a sliding-mode controller for tracking servo of optical disk drives. The tracking servo is majorly subject to two disturbance sources: radial run-out and shock. The lateral run-out disturbance is mostly repeatable, and a model of such disturbance is incorporated into the controller design to effectively compensate for it. Meanwhile, as a shock disturbance is usually non-repeatable and unpredictable, the sliding-mode controller is employed for its robustness to abrupt perturbations. As a result, a sliding-mode controller design based on the internal model principle is tailored for tracking servo of optical disk drives in order to deal with these two major disturbances. Experimental comparative studies are conducted to investigate the effectiveness of the specially designed controller.

Keywords—Mechatronics, optical disk drive, sliding-mode control, servo systems.

I. INTRODUCTION

DISK drives are important medias for massive data storage, in which pick-up heads need to precisely follow data tracks in order to correctly read/write data stored on disks. However, due to the eccentricity of disks and spindle motors, the track-following system is subject to significant radial run-out disturbance. Another source of disturbance in disk drives is shock disturbance coming from external environment. These two kinds of disturbances greatly deteriorate the tracking precision of the pick-up head and hence the performance of data access. They need to be compensated for by the servocontroller.

The run-out disturbance is generally repeatable and of known period. Adaptive feedforward cancellation (AFC) is an effective method for eliminating a periodic input disturbance, in which the disturbance is simply cancelled by adding the negative of its value at the input of the plant [1]–[8]. Another effective way to compensate for a periodic input disturbance is the repetitive learning control method, of which the basic idea is to refine the current control operation cycle by feeding back the tracking error in the previous cycle [9]–[17]. Actually, both the AFC and the repetitive learning control methods have an internal model principle (IMP) equivalent [18]. For the tracking servo-systems of optical disk drives, this paper presents an IMP-based integral sliding-mode controller (IMP-ISMC) design [19] that combines the best features of IMP-based and the sliding-mode controller designs, so as to alleviate the

This work was supported by the National Science Council of ROC under NSC 102-2221-E-003-020-MY2.

Yu-Sheng Lu is with the Department of Mechatronic Engineering, National Taiwan Normal University, Taipei 106, Taiwan (phone: +886-2-77343512; fax: +886-2-2358-3074; e-mail: luys@ntnu.edu.tw).

Chung-Hsin Cheng and Shuen-Shing Jan are with the Department of Mechanical Engineering, National Yunlin University of Science & Technology, Yunlin, Taiwan.

adverse effects of both repeatable run-out and abrupt shock disturbances simultaneously. With the incorporation of an appropriate internal model, the IMP ensures asymptotic rejection of corresponding repeatable run-out disturbance. Meanwhile, the invariance property of a sliding mode is suitable to deal with the external unexpected disturbance. The design methodology is validated by presenting experimental results concerning the tracking servo of an optical disk drive.

II. EXPERIMENTAL SETUP OF AN OPTICAL DISK DRIVE

Consider an experimental optical disk drive (ODD) with the schematic diagram shown in Fig. 1. The mechanism is composed of a spindle motor for the rotation of the disk, an optical pick-up head (PUH) for focusing and track-following, and a coarse actuator, usually referred to as the sled motor or the traverse motor and used in combination with a transmission and a linear guide to enable long-stroke motion of the PUH in radial direction orthogonal to the track. The goal of this ODD is to read the data recorded on a track of the disk. To achieve this, the laser spot should be focused on the recorded layer of the disk through an object lens that is actuated in the focus direction shown in Fig. 1 by a voice coil motor in the PUH. In addition, the laser spot needs to be on the track of the disk using a dual-actuator servo mechanism that consists of a sled motor for coarse motion and a voice coil motor for fine motion adjustment both in the radial direction. Because the role of the coarse actuator is simply to move the fine actuator slowly over the operating range, track-following performance depends almost entirely on how well the tracking actuator is controlled. Therefore, only the tracking actuator is considered as the plant in the track-following control system as in the previous studies [20]–[23].

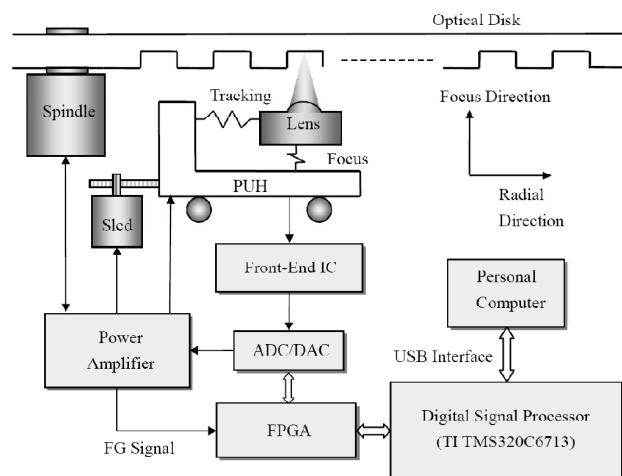


Fig. 1 Schematic of the experimental system [20]

Concerning the electronic portion of the experimental system shown in Fig. 1, a digital phase-locked loop (PLL) is implemented in an FPGA (Field Programmable Gate Array), model XCV100PQ240-C6 from Xilinx, Inc., for controlling the spindle motor at a constant angular velocity. The feedback signal in the spindle servo is the FG signal that has six cycles of square waveform in one motor revolution. The digital servo systems that demand fast responses and thus high sampling frequencies in the ODD are the focus servo and the track-following servo, in which the tracking and the focus error signals are generated by the analog front-end IC, SP3723A from Texas Instruments Incorporated. At the rate of 195.31 kHz, the FPGA samples the tracking and the focus error signals through 10-bit analog-to-digital converters (ADCs) and then generates an interrupt request to the TMS320C6713 digital signal processor (DSP) that is the controller core. In an interrupt service routine, the DSP reads the information on position errors from the FPGA, calculates control algorithms, and sends control efforts to current amplifiers through 12-bit digital-to-analog converters (DACs) and some analog signal processing circuits.

III. SYSTEM MODEL AND CONTROLLER DESIGN

A. Modeling for Controller Design

Due to the present opto-mechanical structure, only the position error can be sensed by the photo diodes whose outputs are processed by current-to-voltage converters and the analog front-end IC, converting the position error to the electrical tracking error signal e with a conversion ratio denoted by k_{PD} . Let the output x and the reference r denote the beam spot and the track positions multiplied by k_{PD} . Only the tracking error described by $e = x - r$ is measurable. The tracking actuator is a voice coil motor driven by a current amplifier and can be approximated by a standard second-order system described by

$$\ddot{x} = -2\zeta\omega_n\dot{x} - \omega_n^2x + b(u + v) \quad (1)$$

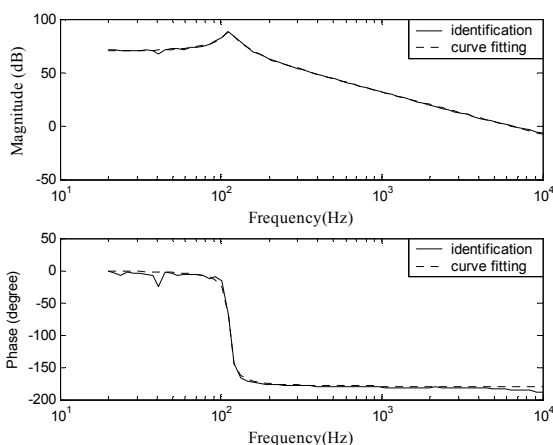


Fig. 2 Swept-sine measurement and curve-fitting

in which ζ is the damping ratio, ω_n is the undamped natural

frequency, u is the scalar control input, b denotes the input gain, and v represents an unknown external disturbance referred to the input. Since only the tracking error signal is available in an ODD, both the system identification and the controller-estimator design have to be performed based on the error signal rather than on the position output signal, and (1) is rewritten as

$$\dot{e} = -2\zeta\omega_n\dot{e} - \omega_n^2e + b(u + d) \quad (2)$$

in which the lumped perturbation $d = v - (\ddot{r} + 2\zeta\omega_n\dot{r} + \omega_n^2r)/b$ that includes the unavailable reference r as a source of perturbation in this error-based model. The lumped perturbation is thus assumed to satisfy $\ddot{d} + \omega_0^2d = 0$, in which ω_0 denotes the disk rotational speed. For identification purpose, a SigLab 20-42 Dynamic Signal Analyzer (DSA) from Spectral Dynamics, Inc., injects an additional known excitation signal into the track-following servo loop. In fact, the DSA automatically steps a sine wave over a specified frequency range and measures the frequency response of the plant. Subsequently, a MATLAB function *invfreqs*(\cdot) performs the least-squares fit to the frequency response data, as shown in Fig. 2. This yields a nominal transfer function of the tracking actuator, giving $\zeta = 0.05$, $\omega_n = 708.80$ rad/s, and $b = 1.543 \times 10^9$. It is seen that the tracking actuator to be controlled is lightly damped with a resonance mode of approximately 113 Hz.

A combined model of plant and exo-system, which contains an internal model whose input is the tracking error, is:

$$\frac{d}{dt} \begin{bmatrix} z_1 \\ z_2 \\ \mathbf{e} \end{bmatrix} = \begin{bmatrix} 0 & 1 & 0 \\ -\omega_0^2 & 0 & \mathbf{C} \\ 0 & 0 & \mathbf{A} \end{bmatrix} \begin{bmatrix} z_1 \\ z_2 \\ \mathbf{e} \end{bmatrix} + \begin{bmatrix} 0 \\ 0 \\ \mathbf{B} \end{bmatrix} (u + d) \quad (3)$$

in which z_1 and z_2 are state variables of the internal model, and the tracking error state vector $\mathbf{e} := [e_1 \ e_2]^T = [e \ \dot{e}]^T$. The system matrices are: $\mathbf{A} = \begin{bmatrix} 0 & 1 \\ -\omega_n^2 & -2\zeta\omega_n \end{bmatrix}$, $\mathbf{B} = [0 \ b]^T$, and $\mathbf{C} = [1 \ 0]$. From this combined model of the plant and the internal model, an SMC is developed to enhance system robustness to unexpected disturbances, while the internal model having infinite gain at the frequency ω_0 forces the tracking error to converge asymptotically.

B. Design of a Switching Function

In designing an SMC, first determine a desired switching function, and then find a sliding control law that is able to constraint system state on the switching hyperplane, that is, to force the predefined switching function to zero. Rewrite (3) as

$$\frac{d}{dt} \begin{bmatrix} \bar{\mathbf{e}} \\ e_2 \end{bmatrix} = \begin{bmatrix} 0 & 1 & 0 & \dots & 0 \\ -\omega_0^2 & 0 & 1 & \dots & 0 \\ 0 & 0 & 0 & \dots & 1 \\ 0 & 0 & -\omega_n^2 & \dots & -2\zeta\omega_n \end{bmatrix} \begin{bmatrix} \bar{\mathbf{e}} \\ e_2 \end{bmatrix} + \begin{bmatrix} 0 \\ 0 \\ 0 \\ b \end{bmatrix} (u+d) \quad (4)$$

where $\bar{\mathbf{e}} = [z_1 \ z_2 \ e_1]^T \in \mathfrak{R}^3$. With this state partition, the joined model (4) can be divided into two parts as follows:

$$\frac{d}{dt} \bar{\mathbf{e}} = \begin{bmatrix} 0 & 1 & 0 \\ -\omega_0^2 & 0 & 1 \\ 0 & 0 & 0 \end{bmatrix} \bar{\mathbf{e}} + \begin{bmatrix} 0 \\ 0 \\ 1 \end{bmatrix} e_2 \quad (5)$$

$$\frac{d}{dt} e_2 = -2\zeta\omega_n e_2 - \omega_n^2 e_1 + b(u+d) \quad (6)$$

Equation (5) describes the null space dynamics while (6) represents the range space dynamics. In designing an SMC, the variable x_n in (5) is regarded as a control input to the null space dynamics and should be so assigned that the null space dynamics is shaped to the desired sliding dynamics. Let

$$e_2 = -\lambda \bar{\mathbf{e}} \quad (7)$$

where $\lambda = [\lambda_1 \ \lambda_2 \ \lambda_3]$ being a constant row vector to be determined. The state feedback with feedback gains λ can place the poles of the null space dynamics to any desired locations only when the null space dynamics is completely controllable. Since the plant is completely controllable and have no zeros at $\pm i\omega$, the null space dynamics is completely controllable, and any linear state feedback method can be utilized to determine λ [19]. Several approaches have been developed for the linear state feedback, including linear quadratic minimization [24] and direct eigenvalue assignment [25].

To shape the null space dynamics, the state variable e_2 should be constrained to maintain the validity of (7). According to (7), define the switching function

$$\sigma(t) = s(t) + k \int_0^t s(\tau) d\tau \quad (8)$$

where $s = e_2 + \lambda \bar{\mathbf{e}}$ and k is an integral gain. The introduction of an integral action in the switching function is to suppress an offset error in the plant's output caused by a constant disturbance.

C. Design of a Sliding Control Law

The objective of a sliding control law is to attract system state onto the switching hyperplane so that system state reaches the switching hyperplane and stays on it thereafter. This can be achieved by designing a control law that satisfies the sliding condition, $\sigma(t)\dot{\sigma}(t) < 0$. Taking the derivative of the switching function (8) with respect to time and substituting (6) yields

$$\dot{\sigma} = \dot{e}_2 + \lambda \dot{\bar{\mathbf{e}}} + ks = \dot{e}_2 + \eta \quad (9)$$

where $\eta = \lambda \left(\begin{bmatrix} 0 & 1 & 0 \\ -\omega_0^2 & 0 & 1 \\ 0 & 0 & 0 \end{bmatrix} \bar{\mathbf{e}} + \begin{bmatrix} 0 \\ 0 \\ 1 \end{bmatrix} e_2 \right) + ks$. Dividing both sides

of (17) by b and substituting (8) into the resulting equation gives

$$b^{-1} \dot{\sigma} = -b^{-1} (2\zeta\omega_n e_2 + \omega_n^2 e_1) + u + d + b^{-1} \eta \quad (10)$$

which leads to the IMP-ISMC law

$$u = b^{-1} (2\zeta\omega_n e_2 + \omega_n^2 e_1 - \eta) - D \operatorname{sgn}(\sigma) \quad (11)$$

where $\operatorname{sgn}(\cdot)$ denotes the discontinuous sign function, and D denotes a positive switching gain that is assumed to be greater than the magnitude of the lumped disturbance, d . Since b^{-1} is positive for this system, it can be easily verified that the sliding control law (11) ensures the satisfaction of the sliding condition $\sigma(t)\dot{\sigma}(t) < 0$ for $\sigma(t) \neq 0$ and $t \geq 0$, guaranteeing the existence of the sliding mode and thus robust performance of the closed-loop system.

IV. EXPERIMENTAL EVALUATION

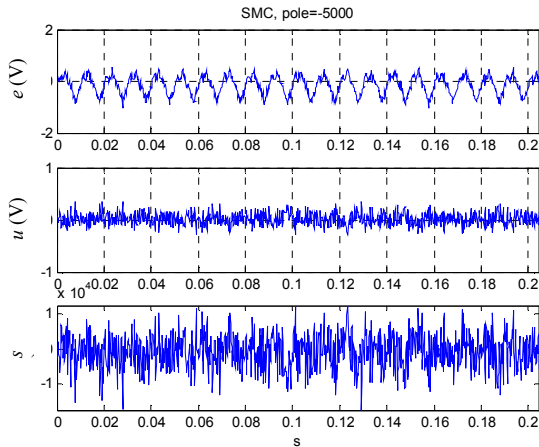
A. Controller Design for Comparison Study

The design procedures of both the conventional sliding-mode controller (SMC) and the conventional linear IMP-based controller can be found in [26], [27], respectively. In addition to the IMP-ISMC, both the conventional SMC and the linear IMP-based controller are designed and implemented for comparison study. In the following experiments, an ordinary DVD-ROM disk is used, and the rotational speed of the spindle motor is 6000 rpm, i.e., 100 Hz, leading to $\omega_0 = 200\pi$ rad/s. Moreover, for both conventional SMC and the IMP-ISMC, the boundary-layer method [28] with a layer width of 1.5×10^4 is employed to alleviate chattering. Three controllers are designed so that all eigenvalues of the closed-loop systems are equal to -5000 .

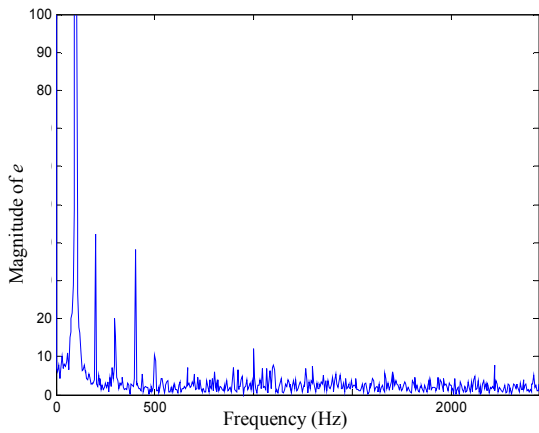
B. Experiments without Artificial Disturbances

Fig. 3 shows the dynamic responses with the SMC, including the spectrum of the tracking error. From both the time response and the spectrum analysis, it can be seen that the tracking error is much influenced by the periodic run-out whose fundamental frequency is 100 Hz. Moreover, there is a significant *dc* component in the tracking error. Fig. 4 shows the dynamic responses with the linear IMP-based controller, including the magnitude spectrum of the tracking error. It can be seen that the major component of the repeatable run-out, whose frequency is 100 Hz, almost have no influence on the tracking error, but there exists a certain amount of *dc* tracking error because the internal model does not include the model of a constant. Fig. 5 shows the dynamic responses with the IMP-ISMC, including

the magnitude spectrum of the tracking error. From Fig. 5, it can be seen that both the dc and the fundamental component of run-out nearly vanishes from the tracking error with the IMP-ISM. Compared with the SMC, the IMP-ISM is robust to the run-out with the help of the internal mode. When compared with the IMP, the IMP-ISM is not only robust to the fundamental component of run-out but also increases insensitivities to other components of run-out.



(a)



(b)

Fig. 3 (a) Dynamic response with the conventional SMC (b) Spectrum of the corresponding tracking error

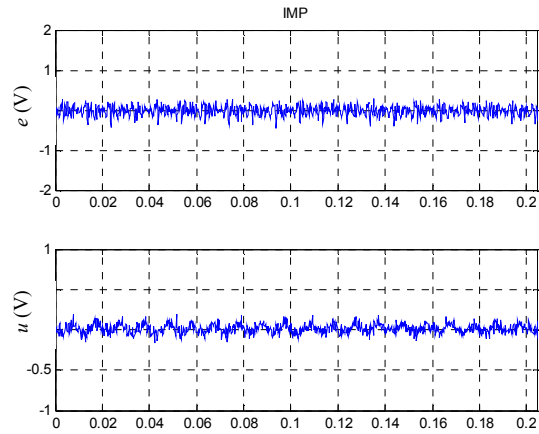
C. Experiments with an Artificial Disturbance

An additional disturbance is introduced to the plant’s input and is described by:

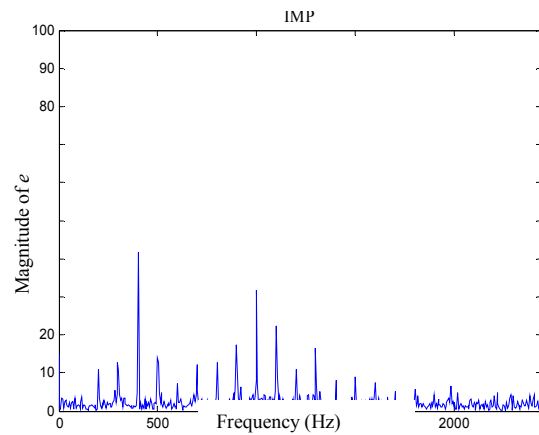
$$d(t) = 0.15[H(t - 0.01536) - H(t - 0.015872)] \quad (12)$$

where $H(\cdot)$ denotes the unit step function. Figs. 6-8 show the dynamic responses to this additional disturbance with the conventional SMC, the linear IMP-based controller, and the IMP-ISM, respectively. It should be noted that the tracking servo with the conventional IMP is unable to continue following the data track after the additional disturbance is

injected into the system. From these figures, it can be seen that the IMP-ISM outperforms the conventional SMC and the linear IMP-based controller in terms of the simultaneous insensitivities to both the repeatable run-out and the additional shock-like disturbances.

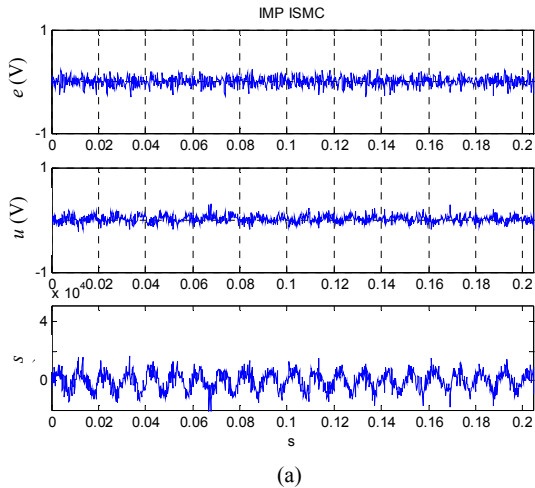


(a)

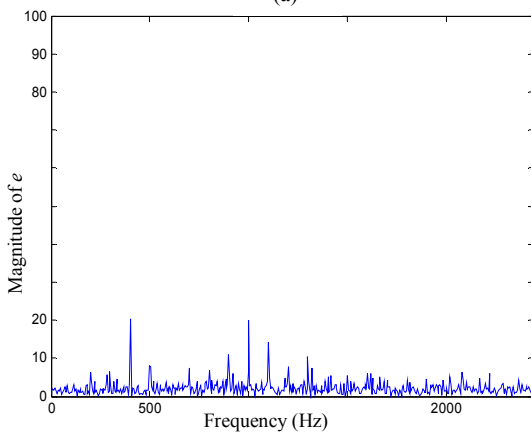


(b)

Fig. 4 (a) Dynamic response with the linear IMP-based controller (b) Spectrum of the corresponding tracking error



(a)



(b)

Fig. 5 (a) Dynamic response with the IMP-ISM (b) Spectrum of the corresponding tracking error

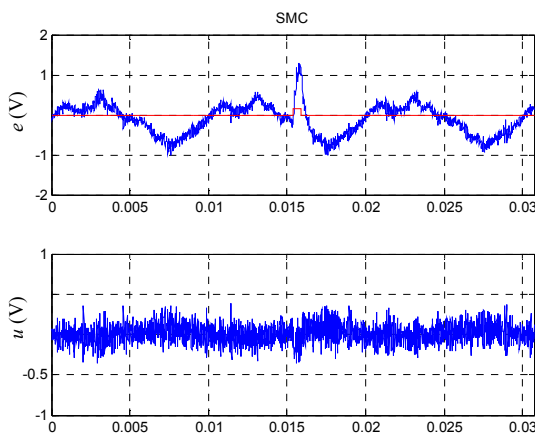


Fig. 6 Response to an additional disturbance with the conventional SMC

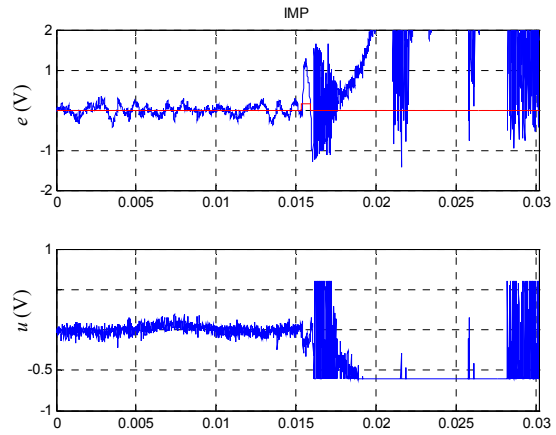


Fig. 7 Response to an additional disturbance with the linear IMP-based controller

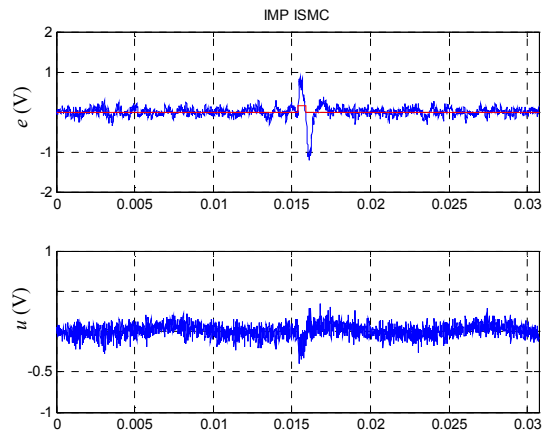


Fig. 8 Response to an additional disturbance with the IMP-ISM

V. CONCLUSION

For the track-following servo-systems of optical disk drives, an integral sliding-mode controller was designed based on the well-known internal model principle (IMP), which combines the best features of the sliding mode and the IMP-based designs. These features are the invariance property from the sliding-mode technique and the asymptotic rejection of disturbances satisfying the internal model. These two salient features are just suitable for dealing with the run-out and shock disturbances that constitute the major disturbance in the track-following servo-systems. The designed controller has been experimentally compared with the conventional sliding-mode controller and the linear IMP-based controller. Experimental results are consistent with the theories that are the basis of the proposed design, and suggest that the sliding-mode increases the system insensitivity to a shock-like disturbance while the incorporation of the internal model effectively alleviates the influences of run-out on the tracking error.

REFERENCES

- [1] M. Bodson, A. Sacks, and P. Khosla, "Harmonic generation in adaptive feedforward cancellation scheme," *IEEE Trans. Automat. Contr.*, vol. 39, no. 9, pp. 1939–1944, 1994.
- [2] W. Messner and M. Bodson, "Design of adaptive feedforward controllers using internal model equivalence," in *Proc. Am. Control Conf.*, Maryland, 1994, pp. 1619–1623.
- [3] A. Sacks, M. Bodson, and W. Messner, "Advanced methods for repeatable runout compensation," *IEEE Trans. Magn.*, vol. 31, no. 2, pp. 1031–1036, 1995.
- [4] S. Weerasooriya, J. L. Zhang, and T. S. Low, "Efficient implementation of adaptive feedforward cancellation in a disk drive," *IEEE Trans. Magn.*, vol. 32, no. 5, pp. 3920–3922, 1996.
- [5] J. L. Zhang, R. Chen, G. Guo, and T. S. Low, "Modified adaptive feedforward runout compensation for dual-stage servo system," *IEEE Trans. Magn.*, vol. 36, no. 5, pp. 3581–3584, 2000.
- [6] M. Tomizuka, "Zero phase error tracking algorithm for digital control," *J. Dyn. Syst. Meas. Control, Trans. ASME*, vol. 109, pp. 65–68, 1987.
- [7] H. S. Lee, "Implementation of adaptive feedforward cancellation algorithms for pre-embossed rigid magnetic (PERM) disks," *IEEE Trans. Magn.*, vol. 33, no. 3, pp. 2419–2423, 1997.
- [8] M. F. Byl, S. J. Ludwick, and D. L. Trumper, "A loop shaping perspective for tuning controllers with adaptive feedforward cancellation," *Precis. Eng.*, vol. 29, pp. 27–40, 2000.
- [9] S. Hara, Y. Yamamoto, T. Omata, and M. Nakano, "Repetitive control system: A new type servo system for periodic exogenous signals," *IEEE Trans. Automat. Contr.*, vol. 33, pp. 659–668, 1988.
- [10] Y. Hamada and H. Otsuki, "Repetitive learning control system using disturbance observer for head positioning system of magnetic disk drives," *IEEE Trans. Magn.*, vol. 32, pp. 5019–5021, 1996.
- [11] K. K. Chew and M. Tomizuka, "Digital control of repetitive errors in disk drive systems," *IEEE Contr. Syst. Mag.*, vol. 10, pp. 16–19, 1990.
- [12] M. Steinbuch, S. Weiland, and T. Singh, "Design of noise and period-time robust high-order repetitive control, with application to optical storage," *Automatica*, vol. 43, no. 12, pp. 2086–2095, 2007.
- [13] M.-C. Tsai and W.-S. Yao, "Analysis and estimation of tracking errors of plug-in type repetitive control system," *IEEE Trans. Automat. Contr.*, vol. 50, no. 8, pp. 1190–1195, 2005.
- [14] Jung-Ho Moon; Moon-Noh Lee; Myung-Jin Chung, "Repetitive control for the track-following servo system of an optical disk drive," *IEEE Trans. Control Systems Technology*, vol. 6, no. 5, pp. 663–670, Sep. 1998.
- [15] K. Chang, I. Shim, and G. Park, "Adaptive repetitive control for an eccentricity compensation of optical disk drivers," *IEEE Trans. Consumer Electronics*, vol. 52, no. 2, pp. 445–450, May 2006.
- [16] J. Leyva-Ramos, M. G. Ortiz-Lopez, and L. H. Diaz-Saldierna, "Disturbance Rejection Control Scheme for Optical Disk Drive Systems," *IEEE Trans. Magn.*, vol. 46, no. 10, pp. 3772–3777, Oct. 2010.
- [17] Y. Onuki and H. Ishioka, "Compensation for repeatable tracking errors in hard drives using discrete-time repetitive controllers," *IEEE-ASME Trans. Mechatron.*, vol. 6, no. 3, pp. 132–136, Jun. 2001.
- [18] B. A. Francis and W. M. Wonham, "The internal model principle of control theory," *Automatica*, vol. 12, no. 5, pp. 457–465, 1976.
- [19] Y. S. Lu, "Sliding-mode control based on internal model principle," *Journal of Systems and Control Engineering, Proc. Inst. Mech. Eng. Part I*, vol. 221, no. 3, pp. 395–406, 2007.
- [20] Y. S. Lu and Y. T. Li, "Design of a sliding perturbation estimator with bound estimation," in *Proc. IEEE VSS'08*, Antalya, Turkey, Jun. 8–10, 2008, pp. 308–313.
- [21] M. Heertjes and M. Steinbuch, "Stability and performance of a variable gain controller with application to a dvd storage drive," *Automatica*, vol. 40, pp. 591–602, 2004.
- [22] K. Yang, Y. Choi, and W. K. Chung, "On the tracking performance improvement of optical disk drive servo systems using error-based disturbance observer," *IEEE Trans. Ind. Electron.*, vol. 52, no. 1, pp. 270–279, 2005.
- [23] T. H. Akkermans and S. G. Stan, "Digital servo IC for optical disc drives," *Control Eng. Pract.*, vol. 9, pp. 1245–1253, 2001.
- [24] V. I. Utkin and K.-K. D. Young, "Methods for constructing discontinuity planes in multidimensional variable structure systems," *Automation and Remote Control*, vol. 39, pp. 1466–1470, 1978.
- [25] J. Ackermann and V. I. Utkin, "Sliding mode control design based on Ackermann's formula," *IEEE Trans. Automat. Contr.*, vol. 43, pp. 234–237, 1998.
- [26] Y. S. Lu and J. S. Chen, "A global sliding mode controller design for motor drives with bounded control," *International Journal of Control*, vol. 62, no. 5, pp. 1001–1019, 1995.
- [27] G. F. Franklin, J. D. Powell, and E.-N. Abbas, *Feedback Control of Dynamic System*. NJ: Pearson, 2009.
- [28] J.-J. E. Slotine and W. Li, *Applied Nonlinear Control*. Englewood Cliffs: Prentice-Hall, 1991.